On Coherency Requirements in Steered Beam Adaptive Antenna Systems

Sven Petersson* and Aare Mällo
Antenna Research Center Radio Network Development,
Ericsson AB, SE-431 84 Mölndal, Sweden.
*Phone: +46-31-7473583. Fax: +46-31-7473993. Email: sven.petersson@ericsson.com

***Abstract**: The effect of array errors (amplitude-, phase- and time errors) on the ensemble average directivity of an adaptive antenna array is studied using Monte-Carlo simulations. It is shown that the effect of the errors can be reduced by introducing a so-called Butler matrix close to the radiating elements of the antenna.*

1 Introduction

Adaptive antenna arrays is a means to improve the performance of mobile communication systems by decreasing the cochannel interference, resulting in an increased spectral efficiency and an increased trunking efficiency [2]. However, to achieve the desired performance gain it is necessary that the entire signal chain is properly calibrated, certainly during production, and typically also during normal operation

In this paper Monte-Carlo simulations are used to investigate the effect of calibration errors (amplitude-, phase- and time errors) on the average azimuthal directivity pattern of a steered beam antenna system. The directivity is chosen as a suitable performance measure since it does not require us to specify a complex traffic model. Also, since time errors are included in the present model, simulations are chosen as the simplest tool of evaluation. The effect of amplitude- and phase errors only can be described analytically as shown in reference [1], but with time errors present the analytical approach becomes more complicated.

To illustrate the effect of array errors three model systems, A, B and C, are considered here (Figure 1). System A is an ideal array without any errors. System B is a non-ideal array with errors present, and finally, system C is a non-ideal array with a Butler matrix placed close to the radiating elements in the antenna. It is assumed that the Butler matrix together with the antenna elements forms a perfectly coherent subsystem. The array errors are assumed to be independent, and introduced in the feeder cables as shown in Figure 1.

The purpose of the Butler matrix in system C is to reduce the effect of array errors. This is indeed the result, and, as will be shown later in this report, in some directions the presence of the Butler matrix will even nullify the effect of array errors.

The outline of this paper is as follows. In section 2 analytical expressions for the *instantaneous*, azimuthal directivity (IAD) of the three model systems in Figure 1 is derived. In section 3 these analytical expressions are taken as a starting point for calculating a time and ensemble average of the IAD using Monte-Carlo simulations. Finally, in section 4 a short discussion and a summary of the results are given.

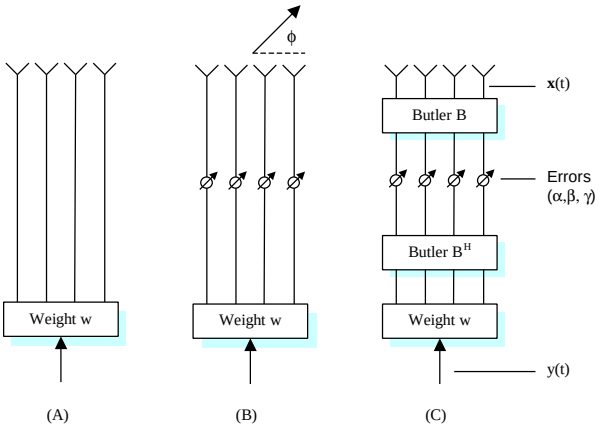

Figure 1. The three model systems considered in this paper. (A): Ideal antenna array without errors, (B): Non-ideal array with errors, and (C): Non-ideal array with errors and with a Butler matrix "B" close to the radiating elements. In the figure f denotes the azimuth angle, $y(t)$ is the baseband signal, $\mathbf{w}$ is an adaptive (complex) weight vector that is used to shape the antenna pattern, and $\mathbf{x}(t)$ is the antenna excitation vector. Parameters a, b and g represent the errors in amplitude, phase and time, respectively.

2 Model

2.1 Instantaneous directivity

The instantaneous, azimuthal directivity (IAD) for an antenna array at time t is defined as

$$D(\theta,\phi,t) \equiv 2\pi F(\theta,\phi,t) / P_{rad}(\theta,t) \tag{2.1}$$

where $F(\theta,\phi,t)$ is the radiated power per unit solid angle in direction $\{\theta,\phi\}$, and $P_{rad}(\theta,t)$ is the total radiated power per radian in elevation angle θ,

$$P_{rad}(\theta,t) \equiv \int_0^{2\pi} F(\theta,\phi,t)\,d\phi \tag{2.2}$$

The radiated power F can be written as

$$F(\theta,\phi,t) = |G(\theta,\phi,t)|^2 \tag{2.3}$$

where G is the complex, antenna far-field pattern,

$$G(\theta,\phi,t) = g_e(\theta,\phi)\,g_a(\theta,\phi,t) \tag{2.4}$$

and g_e and g_a are the element- and the array-patterns, respectively. The element-pattern itself is not of particular interest here, and we simply assume that it has a sinusoidal shape, and that it is directed in the positive y-direction,

$$g_e(\theta,\phi) = \begin{cases} \sqrt{2/\pi}\,\sin(\phi), & 0 \le \phi \le \pi \\ 0, & \text{else} \end{cases} \tag{2.5}$$

The array-pattern can be written as

$$g_a(\theta,\phi,t) = \mathbf{s}^{\mathrm{H}}\mathbf{x}(t) \tag{2.6}$$

where $(\cdot)^{\mathrm{H}}$ denotes the Hermit conjugate, $\mathbf{x}(t)$ is the L-dimensional antenna excitation vector, and $\mathbf{s}$ is a short-hand notation for a steering vector in direction $\{\theta,\phi\}$,

$$\mathbf{s}^{\mathrm{T}} = [s_1, s_2, \cdots s_L] \tag{2.7}$$

$$s_k = s_k(\theta,\phi) = \exp\{i2\pi f_c t_k(\theta,\phi)\} \tag{2.8}$$

In eqs. (2.7-8) $(\cdot)^{\mathrm{T}}$ denotes matrix transpose, L is the number of antenna elements, f_c is the carrier frequency, and t_k is the time delay for a plane wave traveling from antenna element number k, measured relative to the origin,

$$t_k(\theta,\phi) = \mathbf{r}_k \cdot \hat{n}(\theta,\phi)/c \tag{2.9}$$

where c is the speed of light, $\hat{n}(\theta,\phi)$ is the unit vector in direction $\{\theta,\phi\}$, and $\mathbf{r}_k$ is the position of antenna element k.

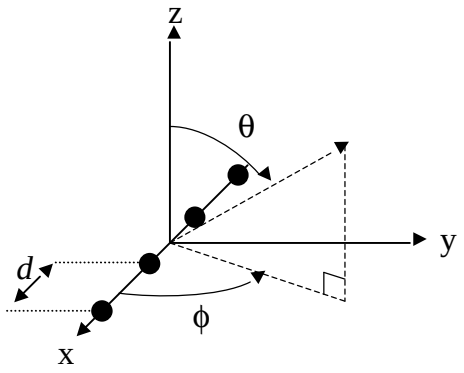

Figure 2. Co-ordinate system. Filled circles indicate the antenna element positions.

Assuming that the antenna elements are located on the x-axis with equal separation d (see Figure 2), the position vector is given by

$$\mathbf{r}_k^{\mathrm{T}} = [d(k-(L+1)/2),\, 0,\, 0] \tag{2.10}$$

For system C in Figure 1 the antenna excitation vector in eq. (2.6) can be written as

$$\mathbf{x}(t) = BM(t)B^{\mathrm{H}}\mathbf{w} \tag{2.11}$$

where B is the $L \times L$ Butler matrix, and M is a time-dependent, diagonal, $L \times L$ matrix that describes the baseband signal, including the array errors,

$$B_{kl} = \frac{1}{\sqrt{L}} \exp\left\{ i\frac{2\pi}{L}\left(k - \frac{L+1}{2}\right)\left(l - \frac{L+1}{2}\right)\right\} \tag{2.12}$$

$$M_{kl}(t) = P_{kl}G_{kl}(t) \tag{2.13}$$

where P and G are two diagonal matrices,

$$P_{kl} = (1+a_k)\exp\{ib_k\}\delta_{kl} \tag{2.14}$$

$$\begin{aligned} G_{kl}(t) &= y(t-\tau_k)\delta_{kl} \\ &= a\textstyle\sum_{m=-\infty}^{m=+\infty} \exp\{i\phi_m\}h(t-mT_c-\tau_k)\delta_{kl} \end{aligned} \tag{2.15}$$

In eqs. (2.14-15) a_k is the relative amplitude error in feeder cable number k, b_k is the phase error, τ_k is the time delay in signal, δ_{kl} is the delta-function, a is an amplitude factor, T_c is the chip period time, ϕ_m is the phase in the I-Q diagram for the chip at time $t = mT_c$, and $h(t)$ is the impulse-response for the pulse-shaping filter.

In the present work it is assumed that the pulse-shaping filter is a root-raised cosine filter. Then, for $t = 0$,

$$h(t) = 1 + a\,\frac{4-p}{p} \tag{2.16}$$

for $|t| = 1/4a$,

$$h(t) = \frac{a}{\sqrt{2p}}\left[(p-2)\cos\left(\frac{p}{4a}\right) + (p+2)\sin\left(\frac{p}{4a}\right)\right] \tag{2.17}$$

and otherwise,

$$h(t) = \frac{\sin(p(1-a)t) + 4at\cos(p(1+a)t)}{p\left(1-(4at)^2\right)t} \tag{2.18}$$

Note that in eqs. (2.16-18) a is a filter design parameter, not to be confused with the amplitude error a_k in eq. (2.14).

Assuming QPSK modulation, the phase angle j_m in eq. (2.15) can take values

$$j_m \in \left[\frac{p}{4}, \frac{3p}{4}, \frac{5p}{4}, \frac{7p}{4}\right] \tag{2.19}$$

The weight vector $\mathbf{w}$ in eq. (2.11) can be designed in many ways to create a specific antenna pattern [3]. However, to keep things simple it is here assumed that it is designed only to create a plane wave in a given target direction $\{q_0, f_0\}$, that is,

$$\mathbf{w} = \frac{1}{L}\mathbf{s}_0 \equiv \frac{1}{L}\mathbf{s}(q_0, f_0) \tag{2.20}$$

where $\mathbf{s}$ is defined by eqs. (2.7-8).

The so-called array-factor for system (C) in Figure 1 can now be written as

$$\left|g_a(q,f,t)\right|^2 = \mathbf{s}^{\mathrm{H}} B M(t) B^{\mathrm{H}} \mathbf{w}\mathbf{w}^{\mathrm{H}} B M^{\mathrm{H}}(t) B^{\mathrm{H}} \mathbf{s} \tag{2.21}$$

Setting the matrix B in eq. (2.21) equal to the identity matrix we obtain the array factor for system (B),

$$\left|g_a(q,f,t)\right|^2 = \mathbf{s}^{\mathrm{H}} M(t) \mathbf{w}\mathbf{w}^{\mathrm{H}} M^{\mathrm{H}}(t) \mathbf{s} \tag{2.22}$$

and finally, by setting the array errors equal to zero in eq. (2.22), $a_k = b_k = g_k = 0$, we obtain the array factor for the ideal antenna array, (A) in Figure 1,

$$\left|g_a(q,f,t)\right|^2 = \mathbf{s}^{\mathrm{H}} \mathbf{w}\mathbf{w}^{\mathrm{H}} \mathbf{s}\, y(t) y^*(t) \tag{2.23}$$

From eq. (2.23) one can see that for the ideal antenna array both F and P_{rad} on the right-hand side of eq. (2.1) will have the same time-dependence, and hence the IAD will be time-independent. This is also true for system B and C, as long as we only have amplitude and phase errors. However, with time errors present, the IAD will in general be error-, data-, and time dependent. That is, the IAD will depend on the specific array errors that are present, it will depend on the specific chip sequence that is being transmitted, and it will also depend on the sampling time-position at the receiver.

2.2 Average directivity for a specific array

The time and data dependence in the directivity can be removed if the directivity is calculated as an average over a given type of chip sequence distribution, and as a time average over one chip period. In a spread-spectrum communication system the chip sequence will be pseudo-random, and one may therefore assume that the phase angles j_m are randomly picked from the allowed values in eq. (2.19). The average directivity for a *specific* antenna array with a *specific* set of array errors is defined as

$$\overline{D}(q,f) \equiv \overline{E_j\left\{D(q,f,t)\right\}} \tag{2.24}$$

where E_j denotes the expectation with respect to a random chip sequence.

Since $E_j\left\{D(q,f,t)\right\}$ is a periodic function in time, with a period time equal to the chip period T_c, the time average can be calculated as

$$\overline{E_j\left\{D(q,f,t)\right\}} = \int_{-T_c/2}^{+T_c/2} E_j\left\{D(q,f,t)\right\} dt \tag{2.25}$$

2.3 Ensemble average directivity

The exact values of the array errors are in general unknown, and in many cases they can only be treated in a statistical fashion. From a practical point of view it is therefore useful to define the directivity as an *ensemble average*, that is, as an average calculated over a hypothetical collection of antenna arrays. The array errors are then described by their statistical distributions. In the present work we assume that the errors are independent, zero mean normal variables with standard deviations s_a, s_b, and s_g, respectively.

The ensemble average azimuthal directivity, $\tilde{D}$, is defined as

$$\tilde{D}(q,f) \equiv E_{abg}\left\{\overline{D}(q,f)\right\} \tag{2.26}$$

where E_{abg} denotes the expectation with respect to the array error distributions.

3 Monte Carlo simulation results

In this section the ensemble average azimuthal directivity $\tilde{D}$ in eq. (2.26) is estimated using Monte-Carlo simulations. The directivity is estimated for the three model systems A, B and C in Figure 1, and for three different directions of the main lobe in the antenna pattern.

As an example we consider a linear array with $L = 4$ antenna elements with equal separation $d = l / 2$, where l is the carrier wavelength. The intrinsic Butler matrix beams in system C are directed at angles

$$f_k = \arccos\left(\frac{l(L - 2k + 1)}{2dL} \right), \quad k = 1,2,\ldots L \qquad (3.1)$$

that is, in this case at angles 41.4°, 75.5°, 104.5° and 138.6°. In figures 3, 4 and 5 the envelope of the Butler matrix beams is shown as the uppermost, dotted curve.

The pulse-shaping root-raised cosine filter $h(t)$ is described by a roll-on-roll-off factor $a = 0.22$, and the summation over index m on the right-hand side of eq. (2.15) is truncated at $|m| = 3$.

The magnitude of the array errors used in the simulation is chosen to be fairly realistic, and the numerical values are shown in Table 1 below.

The Monte-Carlo estimation of $\tilde{D}$ is straightforward. For a given target (main lobe) direction the weight vector $\mathbf{w}$ is first calculated using eq. (2.20). For each Monte-Carlo run n the matrix $M(t)$ in eq. (2.13) is then calculated for a random chip sequence j_m, $m = -3,-2,\ldots +3$, for a random set of normally distributed array errors, and at a random time t picked from a uniform distribution on the interval $[-T_c / 2, +T_c / 2]$. The instantaneous directivity D_n for system B and system C is after that calculated using eqs. (2.21-22) and (2.1-4). The above procedure is repeated $N = 1000$ times, and the ensemble directivity is finally estimated simply as

$$\tilde{D} = \frac{1}{N} \sum_{n=1}^{N} D_n \qquad (3.2)$$

Table 1. Standard deviations for the array errors.

Parameter	σ_α [-]	σ_β [degrees]	σ_γ [seconds]
Value	0.25	15	$0.1 \times T_c$

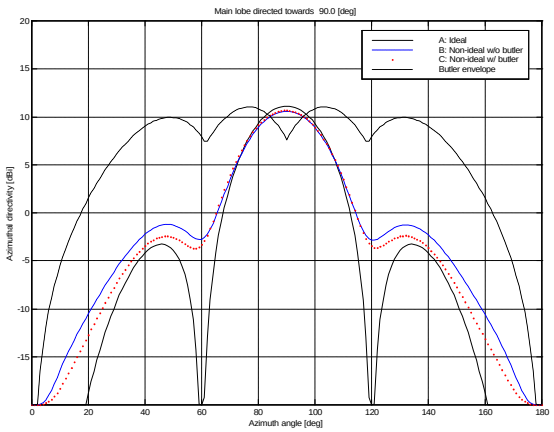

Figure 3. Main lobe directed at 90 degrees, between the second and the third Butler matrix lobe.

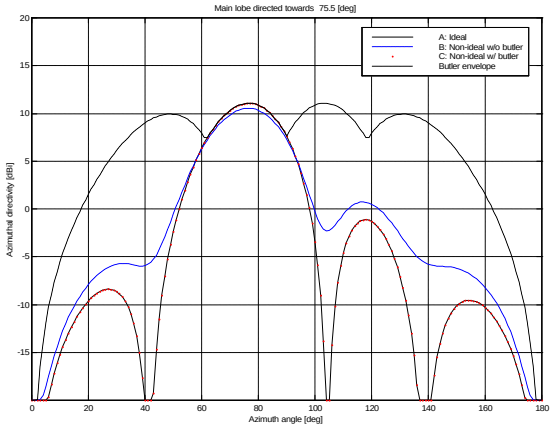

Figure 4. Main lobe directed at at 75.5 degrees, on top of the second Butler matrix lobe.

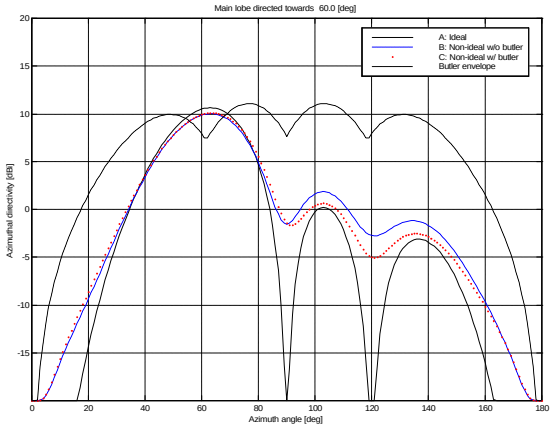

Figure 5. Main lobe directed at 60 degrees, between the first and the second Butler matrix lobe.

In figures 3-5 is shown the ensemble average directivity, estimated using eq. (3.2), and with the variance of the array errors given by Table 1.

In the first plot, Figure 3, the main lobe is directed straight ahead at 90 degrees, in the middle between the second and the third Butler matrix intrinsic lobe. In the figure one can see that the reduction in the main lobe level (MLL) is 0.55 dB for system B, and slightly less, 0.45 dB, for system C. However, the increase in the first side-lobe level (SLL) for system B - roughly 2 dB - is significantly higher than the corresponding value, for system C, 0.85 dB.

In Figure 4 the difference between a system with and without a Butler matrix is shown even more clearly. In this figure the main lobe is directed at 75.5 degrees, on top of the second intrinsic Butler matrix lobe. System C here is effectively immune to the array errors, and displays the same directivity pattern as the ideal array, system A. System B on the other hand shows the same behavior as in the previous figure, the MLL is decreased by 0.5 dB, and the first SLL is increased by 1.8 dB.

Finally, in Figure 5 the main lobe is again placed in the middle between two of the Butler matrix lobes, now at 60 degrees. The overall picture from Figure 3 is repeated for both systems. For system B the MLL is decreased by 0.6 dB, and the first SLL is increased by 1.6 dB. For system C the corresponding numbers are 0.5 dB for the MLL, and 0.4 dB for the first SLL.

Another way to illustrate the benefits of the Butler matrix in system C is shown in table 2, 3 and 4. In those tables we compare the first SLL for system B and C (both measured relative to the SLL for the ideal system) for different magnitudes of the amplitude-, phase-, and time errors. In each table one of the errors is set equal to zero, and the SLL is tabulated as a function of the standard deviation of the two other errors.

The simulations are done in a worst-case situation for system C, with the main lobe directed straight ahead, in the middle between two of the intrinsic Butler lobes.

For the beam direction and the error magnitudes used in table 2-4, the maximum difference in the MLL between system B and C is quite small, around 0.1 dB, and the MLL numbers are therefore not shown here.

As an example of how to read the tables, consider Table 4 on this page. For a phase error $s_b = 20$ degrees and a time error $s_g / T_c = 0.1$, the increase in the SLL is 2.0 dB for system B, and 0.5 dB for system C. That is, the presence of the Butler matrix has reduced the SLL for system C by 2.0 - 0.5 = 1.5 dB.

Table 2. Side-lobe level (SLL) increase in dB for system B and C as a function of amplitude and phase error magnitudes (no time errors present).

			Phase error σ_β [degrees]			
			0	10	20	30
Amplitude error σ_α [-]	0.0	B	0.0	0.4	1.2	2.4
		C	0.0	0.0	0.1	0.4
	0.1	B	0.2	0.4	1.3	2.4
		C	0.1	0.1	0.2	0.5
	0.2	B	0.5	0.7	1.5	2.7
		C	0.3	0.3	0.4	0.7
	0.3	B	1.0	1.3	2.0	3.1
		C	0.6	0.7	0.7	1.0*

Table 3. SLL increase in dB for system B and C as a function of amplitude and time error (no phase errors).

			Time error σ_γ / T_c [-]			
			0.0	0.1	0.2	0.3
Amplitude error σ_α [-]	0.0	B	0.0	1.0	2.1	2.9
		C	0.0	0.3	0.7	1.1*
	0.1	B	0.2	1.1	2.2	3.0
		C	0.1	0.3	0.8	1.2*
	0.2	B	0.5	1.3	2.5	3.2
		C	0.3	0.6	1.0	1.1*
	0.3	B	1.0	1.8	2.9	3.3
		C	0.6	1.0	1.4	1.7*

Table 4. SLL increase in dB for system B and C as a function of phase and time error (no amplitude errors).

			Time error σ_γ / T_c [-]			
			0.0	0.1	0.2	0.3
Phase error σ_β [deg]	0	B	0.0	1.0	2.1	2.9
		C	0.0	0.3	0.6	1.1*
	10	B	0.4	1.2	2.3	3.1
		C	0.0	0.3	0.8	1.2*
	20	B	1.2	2.0	2.8	3.5
		C	0.1	0.5	0.9*	1.3*
	30	B	2.4	3.0	3.8	4.2
		C	0.4	0.8*	1.2*	1.9*

(*) No distinct side-lobe peak found for C – stated value is system C directivity at system B peak position.

4 Summary and conclusions

In this paper we have shown that it is possible to reduce the effects of array excitation errors (amplitude, phase, and time errors) by placing a Butler matrix close to the radiating elements in an antenna array in a steered beam system. In the system with Butler matrix we introduce the errors in beam space, while they are introduced in element space for the system without Butler matrix.

Changes in directivity in the main beam direction as well as for the first sidelobe are studied in systems with and without Butler matrix. Performance for the system with a Butler matrix significantly depends on the main beam direction (whether it is pointed in the direction of a beam defined by the butler matrix or not) while the system without Butler matrix does not show this dependency.

When errors are introduced, the system with Butler matrix shows the largest performance reduction when the main beam is directed in between two intrinsic beams. The gain in directivity in the main beam direction for the system with Butler matrix is for this case very low, on the order of 0.1 dB, compared to the system without Butler matrix. For the side lobe level, the gain using a Butler matrix is more significant, on the order of 1-2 dB for the errors levels considered in this study.

In the most favorable direction for the system with Butler matrix, i.e., when the beam direction equals one of the intrinsic beam directions, the performance gains are significant for main beam directivity as well as for side lobe level.

In conclusion, a steered beam adaptive antenna system with a Butler matrix beamforming network offers potential gains. These can be used either to improve antenna pattern performance for a given error level, or to reduce the coherency requirements for a given pattern performance.

References

[1] B. D. Steinberg, *Principles of Aperture and Array System Design*, New York: Wiley, 1976, ch. 13, pp. 301-316.

[2] L. C. Godara, "*Applications of Antenna Arrays to Mobile Communications, Part I: Performance Improvement, Feasability, and System Considerations*" , Proc. IEEE, vol. 85, no. 7, pp. 1031-1060, July 1997.

[3] L. C. Godara, "*Applications of Antenna Arrays to Mobile Communications, Part II: Beam-Forming and Direction-of-Arrival Considerations*" , Proc. IEEE, vol. 85, no. 8, pp. 1195-1245, August 1997.